

Low-dimensional phases engineering for improving the emission efficiency and stability of quasi-2D perovskite films

Yue Wang(王月), Zhuang-Zhuang Ma(马壮壮), Ying Li(李营), Fei Zhang(张飞), Xu Chen(陈旭), and Zhi-Feng Shi(史志锋)

Citation: Chin. Phys. B, 2021, 30 (**6**): 067802. DOI: 10.1088/1674-1056/abe92b
Journal homepage: http://cpb.iphy.ac.cn; http://iopscience.iop.org/cpb

What follows is a list of articles you may be interested in

Effects of substitution of group-V atoms for carbon or silicon atoms on optical properties of silicon carbide nanotubes

Ying-Ying Yang(杨莹莹), Pei Gong(龚裴), Wan-Duo Ma(马婉铎), Rui Hao(郝锐), and Xiao-Yong Fang(房晓勇)
Chin. Phys. B, 2021, 30 (**6**): 067803. DOI: 10.1088/1674-1056/abdb1e

Optical polarization characteristics for AlGaN-based light-emitting diodes with AlGaN multilayer structure as well layer

Lu Xue(薛露), Yi Li(李毅), Mei Ge(葛梅), Mei-Yu Wang(王美玉), and You-Hua Zhu(朱友华)
Chin. Phys. B, 2021, 30 (**4**): 047802. DOI: 10.1088/1674-1056/abcf3f

Plasmonic properties of graphene on uniaxially anisotropic substrates

Shengchuan Wang(汪圣川), Bin You(游斌), Rui Zhang(张锐), Kui Han(韩奎), Xiaopeng Shen(沈晓鹏, and Weihua Wang(王伟华)
Chin. Phys. B, 2021, 30 (**3**): 037801. DOI: 10.1088/1674-1056/abd168

Modulation of the second-harmonic generation in MoS_2 by graphene covering

Chunchun Wu(吴春春), Nianze Shang(尚念泽), Zixun Zhao(赵子荀), Zhihong Zhang(张智宏), Jing Liang(梁晶), Chang Liu(刘畅), Yonggang Zuo(左勇刚), Mingchao Ding(丁铭超), Jinhuan Wang(王金焕), Hao Hong(洪浩), Jie Xiong(熊杰), and Kaihui Liu(刘开辉)
Chin. Phys. B, 2021, 30 (**2**): 027803. DOI: 10.1088/1674-1056/abd77f

Effects of thermal annealing on the properties of N-implanted ZnS films

Xue Shu-Wen, Zhang Jun, Quan Jun
Chin. Phys. B, 2014, 23 (**5**): 057803. DOI: 10.1088/1674-1056/23/5/057803

Low-dimensional phases engineering for improving the emission efficiency and stability of quasi-2D perovskite films*

Yue Wang(王月), Zhuang-Zhuang Ma(马壮壮), Ying Li(李营),
Fei Zhang(张飞), Xu Chen(陈旭)‡, and Zhi-Feng Shi (史志锋)†

Key Laboratory of Materials Physics of Ministry of Education, School of Physics and Microelectronics, Zhengzhou University, Zhengzhou 450001, *China*

(Received 14 January 2021; revised manuscript received 19 February 2021; accepted manuscript online 24 February 2021)

The two-dimensional (2D) Ruddlesden–Popper-type perovskites, possessing tunable bandgap, narrow light emission, strong quantum confinement effect, as well as a simple preparation method, are identified as a new generation of candidate materials for efficient light-emitting diodes. However, the preparation of high-quality quasi-2D perovskite films is still a challenge currently, such as the severe mixing of phases and a high density of defects within the films, impeding the further promotion of device performance. Here, we prepared the quasi-2D $PEA_2MA_{n-1}Pb_nBr_{3n+1}$ perovskite films by a modified spin-coating method, and the phases with large bandgap were effectively suppressed by the vacuum evaporation treatment. We systematically investigated the optical properties and stability of the optimized films, and the photoluminescence (PL) quantum yield of the treated films was enhanced from 23% to 45%. We also studied the emission mechanisms by temperature-dependent PL spectra. Moreover, the stability of films against moisture, ultraviolet light, and heat was also greatly improved.

Keywords: quasi-2D perovskite films, vacuum evaporation, optical properties, stability

PACS: 78.40.Fy, 78.67.–n **DOI:** 10.1088/1674-1056/abe92b

1. Introduction

The past decades have witnessed the rapid and remarkable development of halide perovskites (ABX_3, $A = MA^+$, FA^+, Cs^+; $B = Pb^{2+}$, $X = Cl^-$, Br^-, I^-) with peculiar photoelectric properties, such as strong optical absorption, low trap state density, and high carrier mobility. Besides the above unique properties, the preparation methods of halide perovskites are also low-cost and facile, and their optical bandgaps and emission wavelengths are tunable by changing the halide compositions. Such properties make halide perovskites have great advantages in the field of photoelectric applications.[1–5] Recently, perovskites-based light-emitting diodes (LEDs) have attracted much attention and their external quantum efficiencies (EQEs) in the green, red, and near-infrared spectral regions have exceeded 20%,[6–8] which opens up a huge opportunity for their actual commercialization. As the emitter layers, the perovskite films obtained by direct spin-coating technology always reveal some inevitable problems, such as a low surface coverage, and a non-uniform morphology with different sized grains. Therefore, improving the crystal quality of perovskite films is one of the effective strategies to boost the EQEs of LEDs. And another strategy is enhancing the radiative recombination of carriers in the emitter layers, which can be successfully achieved by using charge carrier confinement in low-dimensional structures.[9,10]

Very recently, the emerged quasi-2D layered perovskites formed by introducing long organic ligands into the 3D bulk perovskites are expected to achieve high-performance LEDs, which have the advantages of good film morphology, quantum confinement, and high photoluminescence quantum yield (PLQY), as well as enhanced environmental stability.[11–13] In 1994, Era *et al.* firstly reported the 2D layered $(C_6H_5C_2H_4NH_3)_2PbI_4$ LED, which emits the green luminescence centered at 520 nm.[14] But the requirement operating at liquid-nitrogen environment is a challenging issue due to the larger scattering rate at higher temperature. Phenylethylammonium ($PEA = C_8H_9NH_3$) was incorporated into the 3D $MAPbBr_3$ to form the quasi-2D perovskite structure by Sargent's group,[15] and a high-performance LED with EQE of 7.4% was realized after tailoring the energy landscape in the composition of quasi-2D perovskites. In 2018, You *et al.* enhanced the EQE of the green LED to 14.36% by composition and phase engineering, and also the surface passivation.[16] Although numerous efforts have been paid, there is still a lack of significant breakthroughs that propel such LEDs into the commercialization stage.

As we all know, a mixture of multiple phases are usually contained in the quasi-2D perovskites simultaneously,[14] in which the exciton energy of large bandgap phases (small n value) can quickly transfer into the small bandgap phases (large n value), then achieving the final emission band. An excess of small n value ($n = 1$, 2) phases in the quasi-2D

*Project supported by the National Natural Science Foundation of China (Grant Nos. 11774318, 12074347, 12004346, and 61935009) and the Open Fund of State Key Laboratory of Integrated Optoelectronics (Grant No. IOSKL2020KF04).

†Corresponding author. E-mail: shizf@zzu.edu.cn

‡Corresponding author. E-mail: xchen@zzu.edu.cn

© 2021 Chinese Physical Society and IOP Publishing Ltd

perovskites will be adverse to the transfer of the exciton energy, leading to inferior fluorescence efficiency, which is a major obstacle for quasi-2D perovskite LEDs to reach a higher EQE.[17,18] In order to solve this problem, Friend and his co-workers put forward a strategy of an optimized nanocrystal pinning to control the compositions and crystal orientation, and a higher PLQY was obtained after accurate suppression of phases with small n values.[19] In addition, Wang *et al.* proposed a method of washing away excess organic ligands by isopropyl alcohol (IPA), and a significant increase of EQE of quasi-2D perovskite LED from 1.81% to 8.42% was achieved.[20] Besides, Na^+ was introduced into the quasi-2D perovskites to reduce the formation of $n = 1$ phase and a maximum EQE of 11.7% for the sky-blue perovskite LED was acquired.[21]

Taking the above problems into consideration, firstly, we used an anti-solvent crystallization method to prepare the quasi-2D perovskite films, $PEA_2MA_{n-1}Pb_nBr_{3n+1}$. While, the optical properties of the obtained films were relatively poor. Then, the vacuum evaporating solvent before annealing was performed to suppress the phases with small n values. By this way, the PLQY of the quasi-2D perovskite films was significantly enhanced from 23% to 45% through composition engineering strategy. Moreover, the crystallization quality and stability of the films were also greatly improved.

2. Materials and methods

2.1. Materials

Phenylethylammonium bromide (PEABr, 99.99%), methylammonium bromide (MABr, 99.99%), and lead bromide ($PbBr_2$, 99.99%) were purchased from Sigma-Aldrich. N,N-dimethyl formamide (DMF, 99%), dimethyl sulfoxide (DMSO, 99%), and chlorobenzene (CB, 90%) were purchased from Beijing Chemical Reagent Co., Ltd., China.

2.2. Preparation of $PEA_2MA_{n-1}Pb_nBr_{3n+1}$ precursor solution

The 0.5 M $PEA_2MA_{n-1}Pb_nBr_{3n+1}$ precursor solutions were prepared by dissolving PEABr, MABr, and $PbBr_2$ in a mixture of DMF and DMSO (1:1 v/v) at different molar ratios of 2:0:1, 2:1:2, 2:2:3, 2:3:4, and 2:4:5 for the phases with $n = 1, 2, 3, 4, 5$. The solution was then stirred for 12 h at 50 °C until completely dissolved in an argon-filled glove box.

2.3. Characterization

The morphology of the quasi-2D perovskite films was tested using the scanning electron microscopy (SEM) (JSM-7500F). The crystallinity characterization of the $PEA_2MA_2Pb_3Br_{10}$ films was studied by x-ray diffraction (XRD) (Panalytical X'Pert Pro). The steady-state PL and UV-visible absorption spectra of the films were measured by using a steady-state PL spectrum (Horiba; Fluorolog-3) and Shimadzu UV-3150 spectrophotometer at room temperature. The steady-state PL spectra at different temperatures were obtained by using a double grating spectrofluorometer (Horiba; Fluorolog-3), which is equipped with a closed-cycle helium cryostat (Jannis CCS-100). The absolute PLQY of the quasi-2D perovskite films was measured by a fluorescence spectrofluorometer (Horiba; FluoroMax-4) with an integrated sphere with the excitation wavelength of 360 nm (Horiba; Quanta-φ). A pulsed NanoLED was used to conduct the time-resolved PL measurement.

3. Results and discussion

Figures 1(a)–1(c) illustrate the processing procedures for the preparation of 2D perovskite films $PEA_2MA_{n-1}Pb_nBr_{3n+1}$ by using one-step spin-coating method.[22] Firstly, the precursor solution with theoretical stoichiometric ratio was spin-coated on a glass substrate with a low-speed spinning at 500 rpm for 5 s, then a fast-speed spinning at 3000 rpm for 55 s. During the spin-coating process, 100 μL anti-solvent, chlorobenzene, was dropped onto the films in 40 s to assist the crystallization process. Then the sample was directly transferred to the heating plate for annealing treatment at 80 °C for 20 min. Finally, a series of different 2D perovskite compositions $PEA_2MA_{n-1}Pb_nBr_{3n+1}$ (defined by the ratio of chemical formula) were obtained by adjusting the proportion of the precursors. The Ruddlesden-Popper type 2D perovskites $PEA_2MA_{n-1}Pb_nBr_{3n+1}$ are composed of inorganic $[PbBr_6]^{4-}$ layers separated by the organic long chain, $PEA^+((C_6H_2C_2H_4NH_3)^+)$, with small organic cations inserted in the gap of the inorganic layers, which could be seen as a sandwich construction.[23] In the formula $PEA_2MA_{n-1}Pb_nBr_{3n+1}$, n represents the number of lead-based halide octahedra layers, which could be tuned by changing the stoichiometric ratios of precursors. When $n = 1$, pure 2D perovskite $(PEA)_2PbBr_4$ is formed without MA^+ (small cation). With increasing MA^+, quasi-2D compositions ($n = 2$, 3, 4, ..., ∞) are formed, and their luminescence properties are closer to that of 3D perovskite when the value n is larger.

Figure 2 demonstrates the basic characterization of 2D perovskites by XRD, UV-visible absorption, and PL spectra. Figure 2(a) shows the XRD patterns of pure-2D $(PEA)_2PbBr_4$. The single-phase (defined by the inorganic layers of 2D perovskite structure) layered perovskite structure of $n = 1$ composition was confirmed by the strong periodic (00l) planes.[24] Referring to the previous reports, there were always multiple n-phases in the quasi-2D perovskite films,[25,26] which might include $n = 1$, 2, or $n \geq 3$ phases. Specifically, there was only $n = 1$ phase for $n = 1$ composition. While for $n = 2$ quasi-2D perovskite films, we observed the diffraction peak at an angle of 4.0° (identified by triangular symbol in Fig. 2(b)), which is the satellite peak of $n = 2$ phase.[25,27]

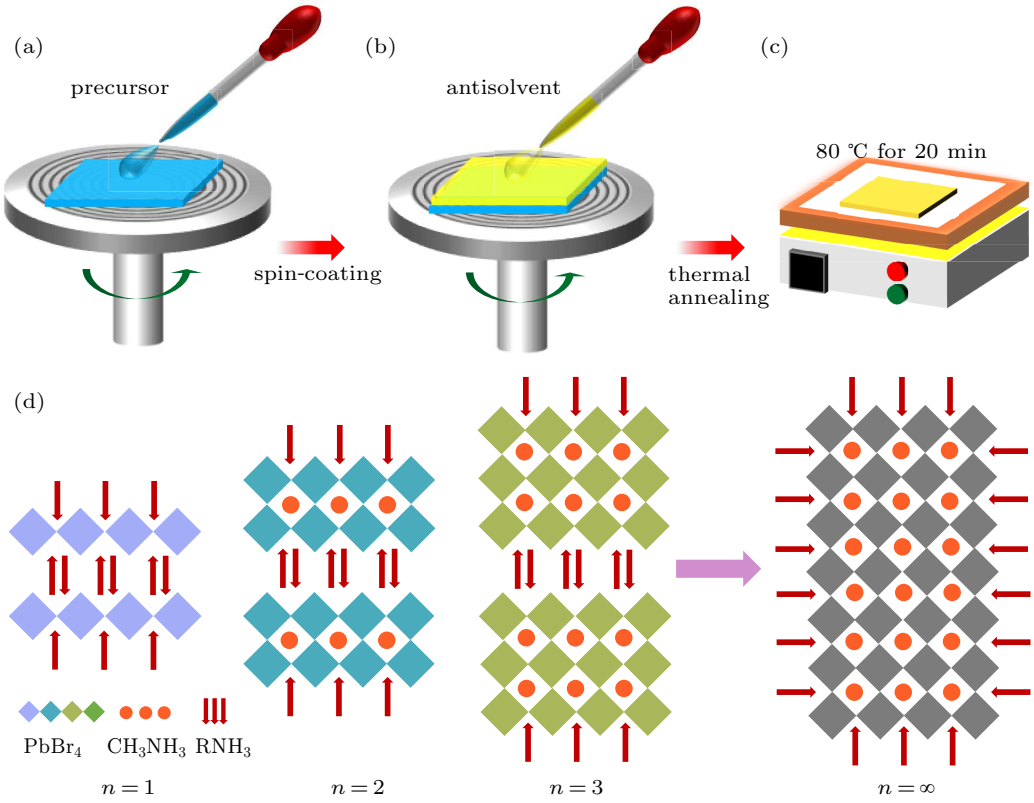


Fig. 1. (a)–(c) Schematic illustration of the preparation of 2D perovskite films by typical one-step spin-coating method. (d) Schematic structures of 2D perovskites, $PEA_2MA_{n-1}Pb_nBr_{3n+1}$, with different phases, $n = 1, 2, 3, \infty$.

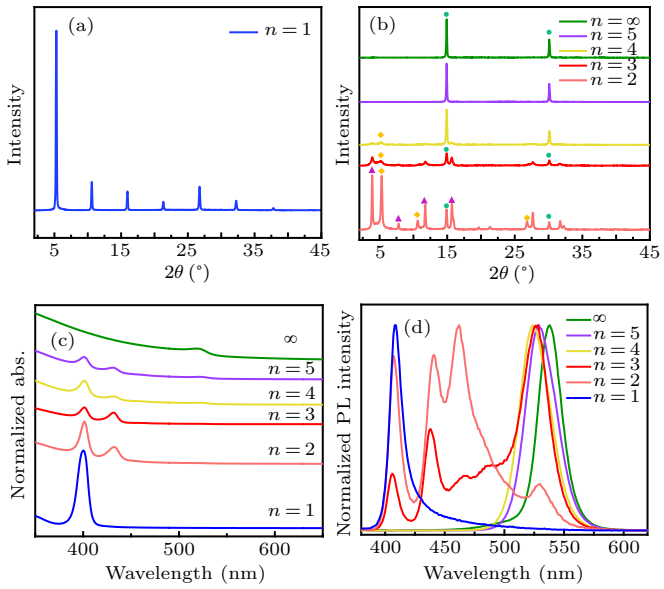


Fig. 2. (a, b) XRD patterns, (c) UV-visible absorption, and (d) steady-state PL spectra of the 2D perovskite films $PEA_2MA_{n-1}Pb_nBr_{3n+1}$ ($n = 1, 2, 3, 4, 5, \infty$) obtained by typical one-step spin-coating method. The diffraction peaks marked by triangles, diamonds, and circles in panel (b) represent the phases of $n = 1$, 2, and ∞, respectively.

In addition to the diffraction peaks of $n = 2$, the diffraction peaks (marked by the diamond) of $n = 1$ phase still remained. With the increase of small cation MA^+, the intensities of diffraction peaks of $n = 1$, 2 phases significantly decrease, and become much weaker in the quasi-2D perovskite with $n = 3$ composition. Until $n \geq 4$ compositions, the diffraction intensities of small angle peaks decline dramatically and even almost absent, which suggests the dominance of $n = \infty$ phase perovskites with negligible phases of small n value in the products. Figure 2(c) presents the evolution of the absorption spectra for different 2D perovskite compositions. It is found that the quasi-2D perovskite films with different compositions have two distinctive absorption peaks located at high-energy states (400 and 431 nm, 3.10 and 2.87 eV) and a low-energy absorption peak (520 nm, 2.38 eV), corresponding to small n and large n ($n = \infty$) phases, respectively, which is consistent with the previous reports.[28,29] While, compared to the absorption of pure 3D perovskite $MAPbBr_3$ (530 nm, 2.34 eV), the low-energy absorption peak (520 nm, 2.38 eV) of the quasi-2D perovskite films shows a blue-shift behavior.

Similar to the measurement results of XRD and UV-visible absorption, a mixture of multiple phases with different n values were also observed in steady-state PL spectra. As shown in Fig. 2(d), the quasi-2D perovskite films display more than two emission peaks due to the existence of multiple phases. For $n = 3$ composition, the quasi-2D perovskite films mainly emit green light and the blue emission greatly decreases. For $n \geq 4$ composition, the blue emission is almost unobservable. An additional observation is that there is an obvious blue-shift of the green emission (525 nm) for the quasi-2D perovskites, compared with the 3D perovskite $MAPbBr_3$ (537.5 nm), which could be attributed to the quantum confinement effect according to the previous reports.[16] Disappoint-

ingly, for $n = 2$ composition, the emission in blue region was much stronger than that in the green region and non-ignorable emission from $n = 1$ and 2 phases was also observed in $n = 3$ composition. It was reported that there is an emission competition between the large bandgap phases (small n phases) and the small bandgap phases ($n = \infty$ phase or 3D perovskite) in the quasi-2D perovskite films.[13,14] The presence of a large number of small compositions ($n = 1$ phase) is not conducive to the efficient energy transition from the quasi-2D perovskite to the 3D perovskite,[29] which would lead to a low fluorescence efficiency.

Therefore, in order to suppress the above small phases (particularly $n = 1$, 2 phases) in the quasi-2D perovskites, we optimized the process of film nucleation by adding a step of vacuum evaporating solvent before annealing, and the vacuum treatment time is 20 min. The detailed procedures are shown in Fig. 3.

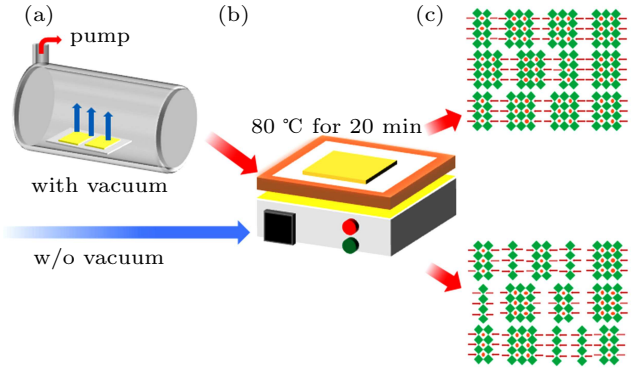


Fig. 3. (a)–(d) Schematic illustration of the improved preparation of 2D perovskite films.

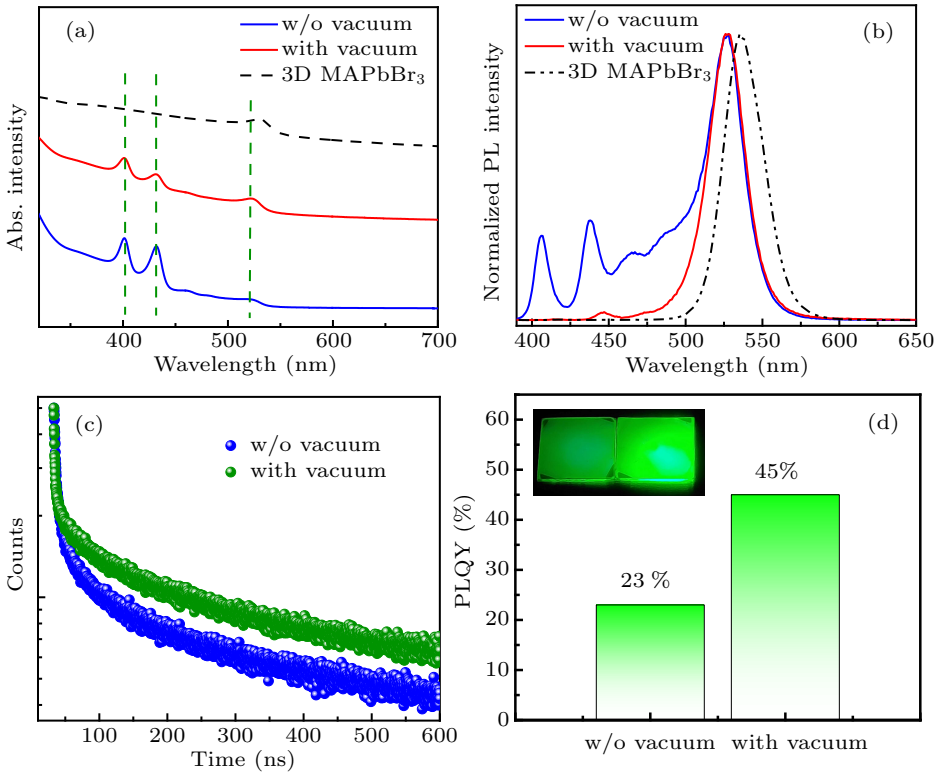


Fig. 4. (a) UV-visible absorption, and (b) steady-state PL spectra of the quasi-2D perovskite films ($n = 3$ composition) with and without the vacuum poling treatment and 3D $MAPbBr_3$ perovskite films (black dashed lines). (c) Time-resolved PL spectra, and (d) PLQYs of the quasi-2D perovskite films ($n = 3$ composition) with and without the vacuum poling treatment. The insets present the corresponding photographs of two quasi-2D perovskite films under 365 nm light illumination (left, control sample; right, treated sample).

At a low pressure of 5 Pa, a rapid evaporation of solvent is beneficial to the crystal nucleation of the quasi-2D perovskites. Then, the sample was annealed at 80 °C for 20 min to improve the crystallinity of the films (called the treated films in the following). Compared with the as-prepared quasi-2D perovskite films ($n = 3$ composition) without the vacuum poling treatment (called the control films), the treated films exhibit a significant improvement in their optical properties. As shown in Fig. 4(a), after the vacuum poling treatment, the intensities of the absorption peaks at 400 nm and 432 nm are significantly suppressed. Analogously, the PL emissions at 410 nm and 440 nm (corresponding to the $n = 1$ and $n = 2$ phases) of the treated films dramatically decline, and the emission at ~ 525 nm dominates the PL spectrum, as seen in Fig. 4(b). Here, it should be mentioned that the dominant emission at ~ 525 nm (Fig. 4(b)) and the absorption at ~ 520 nm (Fig. 4(a)) of the treated films result from the contribution of $n \geq 4$ phases in the quasi-2D perovskite films, because there is an obvious blue-shift trend compared with the pure 3D $MAPbBr_3$ perovskite films (black dashed lines). The above results suggest that an obvious suppression of small n value phases in the quasi-2D perovskite films could be suc-

cessfully achieved by the vacuum poling treatment.

To further investigate the influence of vacuum evaporation solvent on the luminescence properties of the quasi-2D perovskite films ($n = 3$ composition), the time-resolved PL spectra were measured to identify the changes in the carrier recombination dynamics of the control and treated films. As shown in Fig. 4(c), the lifetime decay curves of two samples can be well-fitted by the tri-exponential decay model. For the control films, the longest lifetime $\tau_3 = 197.85$ ns is related to the radiative recombination and the shorter lifetimes $\tau_1 = 2.36$ ns, $\tau_2 = 20.00$ ns can be attributed to the trap-assisted recombination. The obtained PLQY of the control films is measured to be 23% (Fig. 4(d)). After the vacuum evaporation solvent treatment, the longest lifetime τ_3 of the treated quasi-2D perovskite films is increased markedly to 215.26 ns and the PLQY is also significantly improved to 45%. The insets in Fig. 4(d) display the corresponding photographs of the quasi-2D perovskite films with and without the vacuum poling treatment, and significantly different emission intensity can be distinguished. Both the time-resolved PL and PLQY measurement results imply that the effective radiation recombination of the quasi-2D perovskite films was enhanced substantially after the vacuum evaporation solvent treatment. We consider that the obvious promotion of PL lifetime and PLQY for the treated quasi-2D perovskite films is due to the increased amount of large n value phases and the suppression of small n value phases after the vacuum evaporation treatment, and the detailed phase distribution diagrams are illustrated in Fig. 3(c). Many studies have proved that the charge carriers in quasi-2D perovskite films $PEA_2MA_{n-1}Pb_nBr_{3n+1}$ can transfer from small n value phases to large n value phases, leading to an intense green emission. The SEM images in Fig. 5 show the top-view morphology of the control and treated quasi-2D perovskite films. One can see that more compact and pinhole-free films were obtained after vacuum evaporation solvent treatment. So we speculate that another factor for the increased PL lifetime and PLQY of the treated quasi-2D perovskite films is the reduced trap density within the films. Therefore, the vacuum treatment can accelerate the solvent evaporation and nucleation crystallization to form dense films, and the non-radiative recombination centers caused by the defect states were reduced.

To better understand the optical recombination mechanisms of the quasi-2D perovskite films before and after vacuum poling treatment, temperature-dependent PL measurements were conducted (10–300 K). Figures 6(a) and 6(d) show the pseudocolor map of temperature-dependent PL spectra of the quasi-2D perovskite films ($n = 3$ composition) without and with the vacuum poling treatment. One can see that the PL emission of the two films represents a declining trend caused by the thermally activated nonradiative recombination. Meanwhile, the emission peaks exhibit a continuous blue shift with the increasing temperature. Such uncommon blue shift phenomenon may result from the thermal expansion of the crystal lattice and the electron–phonon renormalization.[30–32] The Arrhenius plots of the integrated PL intensities for the control and treated films are shown in Figs. 6(b) and 6(e), and the data could be well fitted by the following formula:[33]

$$I(T) = \frac{I_0}{1 + A\exp\left(-\dfrac{E_B}{k_B T}\right)}, \tag{1}$$

where I_0 is the emission intensity at 0 K and A is a proportional constant, and k_B is the Boltzmann constant. The fitting result demonstrates a value of $E_B = 56.45$ meV for the treated quasi-2D perovskite films (Fig. 6(e)), smaller than that of the control films ($E_B = 62.45$ meV) due to the suppression of phases with small n values, which is consistent with the previous reports.[17,34]

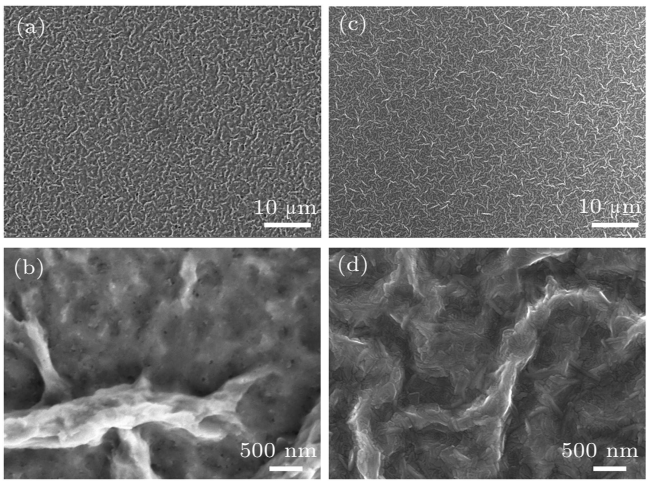


Fig. 5. SEM images of the quasi-2D perovskite films ($n = 3$ composition) without (a), (b) and with (c), (d) the vacuum poling treatment.

In order to examine the exciton–phonon interaction in carrier recombination process, the linewidth broadening behavior of the emission peak was investigated. As seen in Figs. 6(c) and 6(f), the full-width at half-maximum (FWHM) values of the PL emission peaks at different temperatures were fitted by using the following function:[35]

$$\Gamma(T) = \Gamma_0 + \sigma T + \frac{\Gamma_{OP}}{\exp(\hbar\omega_{OP}/KT) - 1}, \tag{2}$$

where Γ_0 is the non-uniform linewidth, σ is the exciton-acoustic phonon interaction, Γ_{OP} is the exciton-optical fitting coefficient, and $\hbar\omega_{OP}$ is the optical phonon energy. According to the equation, a nonlinear increase in FWHM with the increasing temperature mainly results from the contribution of acoustic and optical phonons. Finally, the $\hbar\omega_{OP}$ values of the control and treated films were fitted to be 31.18 meV and

30.12 meV, respectively. Note that the slight decrease of the optical phonon energy suggests that the exciton–phonon interaction in the treated films is relatively weaker. The above results imply that small n value phases with large exciton–phonon interaction were effectively suppressed by the vacuum treatment.

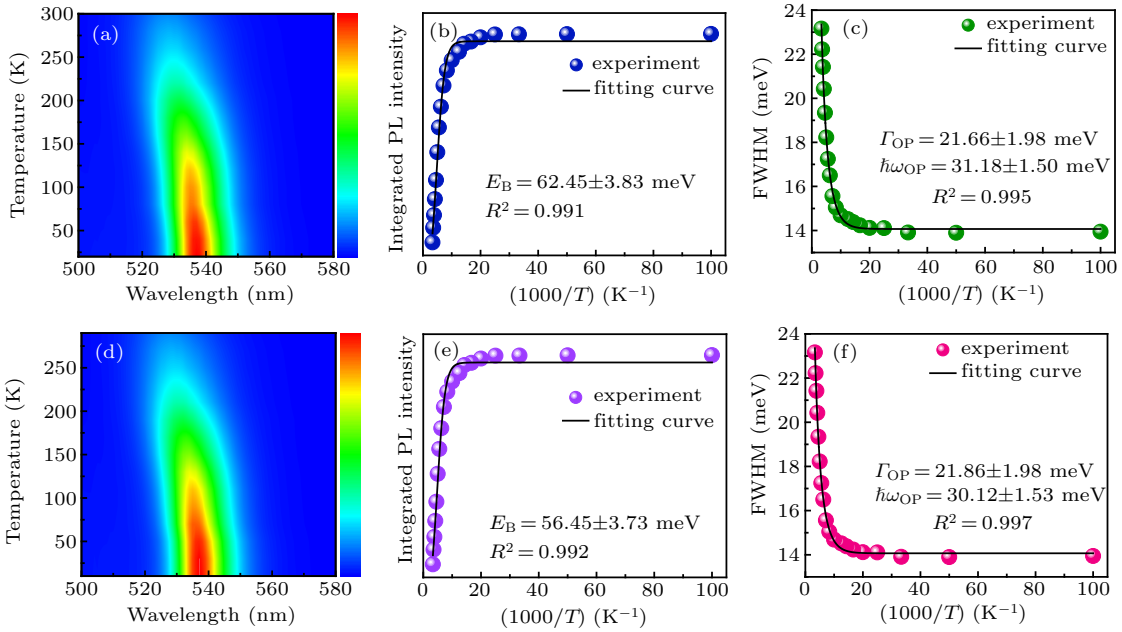


Fig. 6. (a), (d) Pseudocolor map of the temperature-dependent PL spectra of the quasi-2D perovskite films ($n = 3$ composition) without and with the vacuum poling treatment. (b), (e) Integrated PL intensity, and (c), (f) FWHM of the quasi-2D perovskite films ($n = 3$ composition) without and with the vacuum poling treatment.

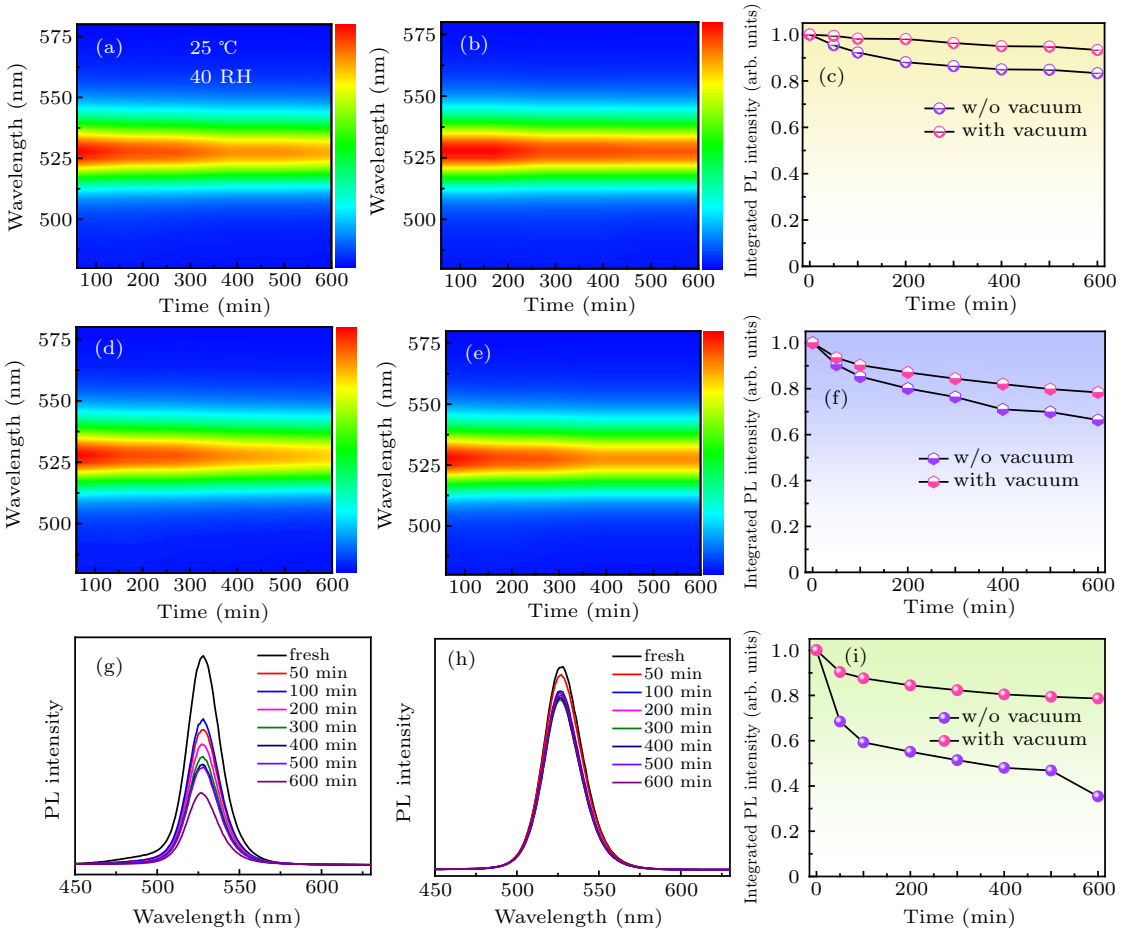


Fig. 7. (a), (b) PL spectra evolution, and (c) PL intensity evolution of the quasi-2D perovskite films without/with the vacuum poling treatment in the air ambient (25 °C, 40% humidity). (d)–(f) Photostability test of the quasi-2D perovskite films without/with the vacuum poling treatment under continuous UV light irradiation (365 nm, 3.0 mW/cm^2). (g)–(i) Thermal stability test of the quasi-2D perovskite films without/with the vacuum poling treatment under continuous heating at 60 °C for 600 min.

It is particularly notable that the stability of halide perovskites is the main factor affecting their practical commercial applications.[36,37] Typically, the conventional 3D lead-halide perovskites are especially sensitive to the surrounding environment and a rapid decomposition of organic-inorganic hybrid perovskites will occur in moist air due to the hygroscopic amine salts, which will dramatically reduce the fluorescence efficiency. In this study, the environmental stability of the quasi-2D perovskite films was evaluated by exploring the effects of humidity, UV light irradiation, and heat on the optical properties of products without/with vacuum poling treatment. Figures 7(a)–7(c) show the moisture stability of the control and treated films. In the 40% humidity ambient condition (25 °C), the PL emission of the control films gradually decreased, exhibiting a moderate decay of 18% after a storage for 600 min (Figs. 7(a) and 7(c)). While, for the product with vacuum poling treatment, only a tiny emission decay of about 8% was generated (Figs. 7(b) and 7(c)). It is worth nothing that the FWHM and peak position of PL spectra remained almost unchanged for both films throughout the entire test. Compared to the 3D perovskites, the good stability against moisture for the 2D perovskites is mainly due to the hydrophobic organic amine salt. Under the continuous UV light irradiation, the shape and peak position of the PL emission spectra also keep almost the same for both samples. A moderate emission decay of 18% was observed for the treated films (Figs. 7(e) and 7(f)), while a relative large emission decay of about 35% was generated for the control films after the continuous UV light irradiation for 600 min (Figs. 7(d) and 7(f)). Moreover, the quasi-2D perovskite films with vacuum poling treatment also exhibit excellent thermal stability. As seen in Fig. 7(g), the control films experienced a sharp fluorescence quenching under continuous heating at 60 °C, retaining only 32% of the initial intensity after 600 min. By contrast, nearly 78% of the original PL intensity was retained for the treated films over the same time (Figs. 7(h) and 7(i)). The above results suggest that the stability of the quasi-2D perovskite films against moisture, UV light, and heat can be markedly enhanced by the vacuum poling treatment. The remarkable improvement of environmental stability may be attributed to the suppression of multiple small n value phases (typically $n = 1$, 2 phases) and the promotion of crystallization quality of the films. The improved stability of the materials builds a good foundation for their further photoelectronic device application.

4. Conclusions

A series of 2D perovskite films $PEA_2MA_{n-1}Pb_nBr_{3n+1}$ ($n = 1, 2, 3, 4, 5, \ldots, \infty$) were prepared by one-step spin-coating method, and the phases of quasi-2D perovskite films with small n values were significantly restrained by the vacuum poling treatment before annealing. The resulting quasi-2D perovskite films $PEA_2MA_2Pb_3Br_{10}$ emitted mainly green light located at 525 nm, showing a slight blue shift compared with that of the 3D perovskite $MAPbBr_3$. Moreover, the detailed measurements on temperature-dependent steady-state and time-resolved PL exhibit that the E_B decreased and PL lifetime increased after the vacuum treatment, which are due to the suppression of small n phases and the reduced traps and defects within the films. The obtained PLQY was also enhanced from 23% to 45%. In addition, the films with the vacuum poling treatment exhibited an improved stability against heat, moisture, and UV light irradiation. This work provides valuable information for the preparation of high-quality quasi-2D perovskite films, facilitating their applications as emitters for high-performance LEDs.

References

[1] Zhang F, Zhong H Z, Chen C, Wu X G, Hu X M, Huang H L, Han J B, Zou B S and Dong Y P 2015 *ACS Nano* **9** 4533
[2] Li Y, Shi Z, Liang W Q, Wang L, Li S, Zhang F, Ma Z, Wang Y, Tian Y, Wu D, Li X, Zhang Y, Shan C and Fang X S 2020 *Mater. Horiz.* **7** 530
[3] Yang J X, Zhang P, Wang J P and Wei S H 2020 *Chin. Phys. B* **29** 108401
[4] Shen Z H, Song P J, Qiao B, Cao J Y, Bai Q Y, Song D D, Xu Z, Zhao S L, Zhang G Q and Wu Y J 2019 *Chin. Phys. B* **28** 086102
[5] Li Y, Shi Z F, Li X J and Shan C X 2019 *Chin. Phys. B* **28** 017803
[6] Lin K, Xing J, Quan L N, Arquer F P G D, Gong X W, Lu J X, Xie L Q, Zhao W J, Zhang D, Yan C Z, Li W Q, Liu X Y, Lu Y, Kirman J, Sargent E H, Xiong Q H and Wei Z H 2018 *Nature* **562** 245
[7] Cao Y, Wang N N, Tian H, Guo J S, Wei Y Q, Chen H, Miao Y F, Zou W, Pan K, He Y R, Cao H, Ke Y, Xu M M, Wang Y, Yang M, Du K, Fu Z W, Kong D C, Dai D X, Jin Y Z, Li G Q, Li H, Peng Q M, Wang J P and Huang W 2018 *Nature* **562** 249
[8] Shi Z, Li Y, Zhang Y, Chen Y, Li X, Wu D, Xu T, Shan C and Du G 2017 *Nano Lett.* **17** 313
[9] Xing G C, Wu B, Wu X Y, Li M J, Du B, Wei Q, Guo J, Yeow E K L, Sum T C and Huang W 2017 *Nat. Commun.* **8** 14558
[10] Richter J, Abdi-Jalebi M, Sadhana A, Tabachnyk M, Rivett J P H, Pazos-Outón L M, Gödel K C, Price M, Deschler F and Friend R H 2016 *Nat. Commun.* **7** 13941
[11] Cheng L, Jiang T, Cao Y, Yi C, Wang N N, Huang W and Wang J P 2020 *Adv. Mater.* **32** 1904163
[12] Chen Y N, Sun Y, Peng J J, Tang J H, Zheng K B and Liang Z Q 2018 *Adv. Mater.* **30** 1703487
[13] Liu X K and Gao F 2018 *J. Phys. Chem. Lett.* **9** 2251
[14] Era M, Morimoto S, Tsutsui T and Saito S 1994 *Appl. Phys. Lett.* **65** 676
[15] Quan L N, Zhao Y B, Arquer P G F, Sabatini R, Walters G, Voznyy O, Comin R, Li Y Y, Fan J Z, Tan H, Pan J, Yuan M J, Bakr O M, Lu Z H, Kim D H and Sargent E H 2017 *Nano Lett.* **17** 3701
[16] Yang X L, Zhang X W, Deng J X, Chu Z M, Jiang Q, Meng J H, Wang P Y, Zhang L Q, Yin Z G and You J B 2018 *Nat. Commun.* **9** 2
[17] Smith M D, Connor B A and Karunadasa H I 2019 *Chem. Rev.* **119** 3104
[18] Ban M Y, Zou Y T, Rivett J P H, Yang Y G, Thomas T H, Tan Y S, Song T, Gao X Y, Credgington D, Deschler F, Sirringhaus H and Sun B Q 2018 *Nat. Commun.* **9** 1
[19] Lee H D, Kim H, Cho H, Cha W, Hong Y, Kim Y H, Sadhanala A, Venugopalan V, Kim J S, Choi J W, Lee C L, Kim D, Yang H C, Friend R H and Lee T W 2019 *Adv. Funct. Mater.* **29** 1901225
[20] Wang Z B, Wang F Z, Sun W D, Ni R H, Hu S Q, Liu J Y, Zhang B, Alsaed A, Hayat T and Tan Z 2018 *Adv. Funct. Mater.* **28** 1804187
[21] Pang P Y, Jin G R, Liang C, Wang B Z, Xiang W, Zhang D L, Xu J W, Hong W, Xiao Z W, Wang L, Xing G C, Chen J S and Ma D G 2020 *ACS Nano* **14** 11420
[22] Jeon N J, Noh J H, Kim Y C, Kim Y C, Yang W S, Ryu S C and Seok S I 2014 *Nat. Mater.* **13** 897

[23] Ma S, Cai M L, Cheng T, Ding X H, Shi X Q, Alsaedi A, Hayat T, Ding Y and Dai S Y 2018 *Sci. China Mater.* **61** 1257
[24] Liang D, Peng Y L, Fu Y P, Shearer M J, Zhang J J, Zhai J Y, Zhang Y, Hamers R J, Andrew T L and Jin S 2016 *ACS Nano* **10** 6897
[25] Ren Z W, Li L, Yu J H, Ma R M, Xiao X T, Chen R, Wang K, Sun X W, Jin W J and Choy W C H 2020 *ACS Energy Lett.* **5** 2569
[26] Xiao Z G, Kerner R A, Zhao L F, Tran N L, Lee K M, Koh T W, Scholes G D and Rand B P 2017 *Nat. Photon.* **11** 108
[27] Yang X L, Chu Z M, Meng J H, Yin Z G, Zhang X W, Deng J X and You J B 2019 *J. Phys. Chem. Lett.* **10** 2892
[28] Cho H, Jeong S H, Park M H, Kim Y H, Wolf C, Lee C L, Heo J H, Sadhanala A, Myoung N, Yoo S, Im S H, Friend R H and Lee T W 2015 *Science* **350** 1222
[29] Yuan S, Wang Z K, Xiao L X, Zhang C F, Yang S Y, Chen B B, Ge H T, Tian Q S, Jin Y and Liao L S 2019 *Adv. Mater.* **31** 1904319
[30] Shi Z F, Li S, Li Y, Ji H F, Li X J, Wu D, Xu T T, Chen Y S, Tian Y T, Zhang Y T, Shan C X and Du G T 2018 *ACS Nano* **12** 1462
[31] Zhang F, Shi Z F, Ma Z Z, Li Y, Li S, Wu D, Xu T T, Li X J, Shan C X and Du G T 2018 *Nanoscale* **10** 20131
[32] Ma Z Z, Shi Z F, Qin C C, Cui M H, Yang D W, Wang X J, Wang L T, Ji X Z, Chen X, Sun J L, Wu D, Zhang Y, Li X J, Zhang L J and Shan C X 2020 *ACS Nano* **14** 4475
[33] Savenije T J, Ponseca C S, Kunneman L, Abdellah M, Zheng K B, Tian Y X, Zhu Q S, Canton S E, Scheblykin I G, Pullerits T, Yartsev A and Sundström V 2014 *J. Phys. Chem. Lett.* **5** 2189
[34] Wang S, Ma J Q, Li W C, Wang J, Wang H Z, Shen H Z, Li J Z, Wang J Q, Luo H M and Li D H 2019 *J. Phys. Chem. Lett.* **10** 2546
[35] Rudin S, Reinecke T L and Segall B 1990 *Phys. Rev. B* **42** 11218
[36] Ma Z, Shi Z, Wang L, Zhang F, Wu D, Yang D, Chen X, Zhang Y, Shan C and Li X J 2020 *Nanoscale* **12** 3637
[37] Cao Z, Hu F, Man Z, Zhang C, Zhang W, Wang X and Xiao M 2020 *Chin. Phys. Lett.* **37** 127801